

Ultralow Thermal Conductivity in Chain-like TlSe Due to Inherent Tl⁺ Rattling

Moinak Dutta,^a Shidaling Mattheppanavar,^a Matukumilli V. D. Prasad,^b Juhi Pandey,^c Avinash Warankar,^d Pankaj Mandal,^d Ajay Soni,^c Umesh V. Waghmare^{b, e} and Kanishka Biswas^{a, e, *}

^a*New Chemistry Unit, Jawaharlal Nehru Centre for Advanced Scientific Research (JNCASR), Jakkur P.O., Bangalore 560064, India.*

^b*Theoretical Sciences Unit, Jawaharlal Nehru Centre for Advanced Scientific Research (JNCASR), Jakkur P.O., Bangalore 560064, India.*

^c*School of Basic Sciences, Indian Institute of Technology Mandi, Mandi, Himachal Pradesh, 175005, India.*

^d*Department of Chemistry, Indian Institute of Science Education and Research (IISER), Pune 411008, India.*

^e*School of Advanced Materials and International Centre of Materials Science and International Centre of Materials Science, Jawaharlal Nehru Centre for Advanced Scientific Research (JNCASR), Jakkur P.O., Bangalore 560064, India.*

**E-mail: kanishka@jncasr.ac.in*

Experimental & Theoretical Methods.

Synthesis. High quality crystalline TlSe prepared by modified Bridgman technique. Used stoichiometric quantities of high-purity Tl (99.999 %) and Se (99.999 %) (total weight of 5 g) in a quartz ampoule, sealed during high vacuum of 10^{-5} torr. The contents were heated up to 773 K in 6 hr, soaked at this temperature for 6 hr and cooled to crystallization temperature 673 K in 3 hr and soaked for 20 hr and further cooled to room temperature in 6 hr. The obtained product was then finely ground and then Spark Plasma Sintering (SPS) was performed. The Sample was taken in a graphite die of 10 mm diameter. The die was then heated to 250 °C in 5 mins; kept at that temperature for 5 mins and then cooled to room temperature in 10 mins. The pressure was maintained at 3.9 kN throughout the sintering process. We have further synthesized single crystals of TlSe using conventional Bridgman method to compare the thermal conductivity with our highly dense SPS samples. A vacuum sealed ampoule containing stoichiometric amounts of Tl and Se (total 8 g) was heated to 673 K and then was passed through a temperature gradient of 200 K between the two zones at a rate of 1.5mm per hour. The product obtained was then cut using wire cutter and subsequently used for thermal conductivity measurement (Figure S8, SI).

Powder X-ray diffraction (PXRD). PXRD measurements were recorded on Bruker D8 diffractometer using Cu K α ($\lambda = 1.5406$ Å) radiation. Rietveld refinement was carried out using Full prof program.

Thermal conductivity. The thermal diffusivity, D , was measured between 295 K and 525 K using laser flash diffusivity technique in Netzsch LFA-457 instrument. The thermal diffusivity was measured along the parallel and perpendicular to the spark plasma sintering pressed direction. Disc-shaped pellets with *ca.* 10 mm x 2 mm dimensions were used for thermal transport measurement. Total thermal conductivity (κ) (Figure S2, SI) was estimated using the relation, $\kappa =$

$D \times C_P \times \rho$, where ρ is the density (99%) of the sample and C_P is the specific heat capacity at constant pressure measured with respect to Pyroceram reference-standard in Netzsch LFA-457 instrument (Figure S7, SI). Lattice thermal conductivity (κ_L) is extracted by subtracting electronic thermal conductivity (κ_{el}) from total thermal conductivity. κ_{el} is calculated using the Wiedemann Franz law, $\kappa_{el} = L\sigma T$, where σ is the electrical conductivity and L is the temperature dependent Lorentz number. L is calculated using Single Parabolic Band (SPB) model similar to the reference S1. Assuming SPB model Lorentz number (L) is given as:

$$L = \left(\frac{k_B}{e}\right)^2 \frac{3F_0(\eta)F_2(\eta) - 4F_1(\eta)^2}{F_0(\eta)^2}$$

Where, η is the reduced chemical potential and can be obtained by fitting the experimental Seebeck coefficients. k_B represents Boltzmann constant and $F_n(\eta)$ is the n^{th} order Fermi Integral.

Electronic properties. Electrical conductivity (σ) and Seebeck coefficient (S) were simultaneously measured along the SPS pressing direction under He-atmosphere from 295 K up to 525 K using ULVAC-RIKO ZEM-3 instrument. Rectangular bar shaped samples (*ca.* $2 \times 2 \times 8$ mm³) cut from cylindrical samples were used for the electrical measurements.

Band gap measurement. Finely ground sample was used to obtain the optical band gap of the synthesized samples. The optical band gap was estimated in a FT-IR Bruker IFS 66V/S spectrometer within the range of 6000 – 400 cm⁻¹. Absorption (α/S) data were derived using Kubelka-Munk equation: $\alpha/S = (1-R)^2/(2R)$, where R is the reflectance, α and S corresponds to absorption and scattering coefficient, respectively. The energy band gaps were deduced from α/S vs E_g (eV) plot.

Raman spectroscopy. Raman measurement was conducted in back scattering geometry using Horiba Jobin-Yvon LabRAM HR evolution Raman spectrometer with 1800 gr/mm and Peltier

cooled CCD detector. Temperature dependent Raman measurements were performed using Montana cryostat in the range of 4 - 300 K, using 532 nm Unpolarized excitation laser.

THz time-domain spectroscopy (THz-TDS). We have used our home-built THz time-domain spectrometer to record the THz spectrum of TlSe in reflection geometry. The spectrometer is based on a 4 mJ ultrafast (50 fs) amplified laser system. The details of our THz set-up are described elsewhere.^{S2} The use of air-plasma as the THz generation source and employing air-biased coherent detection (ABCD) scheme enables us to extend the spectral range from 0.5 THz to 15 THz. An enclosure continuously purged with dry nitrogen gas avoids THz absorption by water vapour present in ambient air.

In reflection geometry, the reflected THz waveforms are collected and analyzed to determine the dielectric function of the sample.^{S3} In the present experiment, time-domain THz waveforms reflected from a Reference (high resistivity silicon) and the sample (TlSe pallet) are collected in normal incidence. Fourier transformations of the reference and sample THz waveforms and use of Fresnel equation (Eq. 1) for reflection yield the complex refractive index of the sample.

$$\frac{\tilde{E}_{Sample}(\omega)}{\tilde{E}_{Si}(\omega)} = \frac{\frac{\tilde{n}_{sample}-n_{air}}{\tilde{n}_{sample}+n_{air}}}{\frac{n_{si}-n_{air}}{n_{si}+n_{air}}} \quad \text{Eq. 1}$$

Here, $\tilde{E}_{sample}(\omega)$ and $\tilde{E}_{si}(\omega)$ are the reflected THz electric fields in frequency domain from sample and reference (silicon), respectively. \tilde{n}_{sample} , n_{si} and n_{air} are complex/real refractive indices of sample, reference, and dry air, respectively. High resistivity silicon and dry air are nearly non-absorbing media with their refractive indices ($n_{si} = 3.45$ and $n_{air} = 1$) constant over the frequency range of this study. Complex refractive index is written as, $\tilde{n}_{sample} = n + ik$, where n is the real part of the refractive index and k is the extinction coefficient of the sample. Absorption

coefficient (α) is obtained from the relation, $\alpha = 2. \omega. k/c$, where ω is the angular frequency and c is the speed of light.

Computational methods. Electronic and phonon properties are calculated based on the first-principles pseudo potentials within density functional theory (DFT) as implemented in Quantum Espresso code.^{S4} In DFT calculations, we employed generalized gradient approximation (GGA) to the exchange correlation energy functional and used norm-conserving pseudopotentials to treat the interactions between ionic cores and valence electrons, and a plane wave basis with an energy cutoff of 60 Ry (240 Ry) in the representation of the Kohn-Sham wave functions (density). Brillouin zone of the tetragonal unit cell is sampled with a uniform 12x12x12 k-point mesh which is in accordance with Monkhorst-Pack^{S5} scheme. The discontinuity in the occupations number of electronic states near the gap was smeared with Fermi-Dirac distribution functions with a broadening of $k_B T = 0.003$ Ry. Optimized lattice parameters are in agreement with the experimental values.

Calculation of minimum thermal conductivity (κ_{min}). Minimum thermal conductivity was calculated using Cahill's model^{S6} which is given by:

$$\kappa_{min} = \frac{1}{2} \left(\frac{\pi}{6} \right)^{1/3} k_B V^{-2/3} (2v_t + v_l)$$

where k_B denotes Boltzmann constant, V being the average volume per atom, and v_t (1486 m/s and 2101 m/s) and v_l (3471 m/s) denotes mean speed of sound in transverse and longitudinal directions obtained from theoretical calculations by deducing the slope of longitudinal and transverse acoustic phonons in the Γ -X direction. For Γ -X direction, κ_{min} value is to be 0.41 W/mK. For Γ -Z direction the v_t (568 m/s and 568 m/s) and v_l (4378 m/s) values lead to κ_{min} value of 0.32 W/mK.

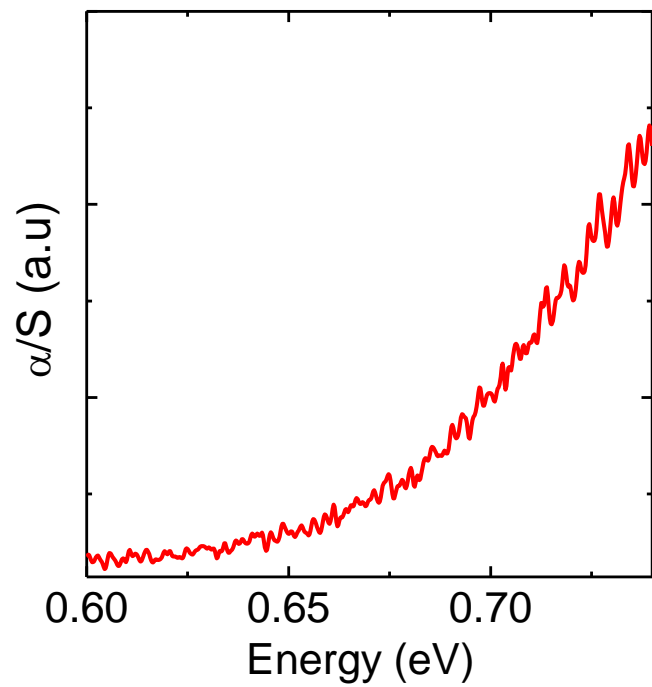


Figure S1. Band gap of TISe.

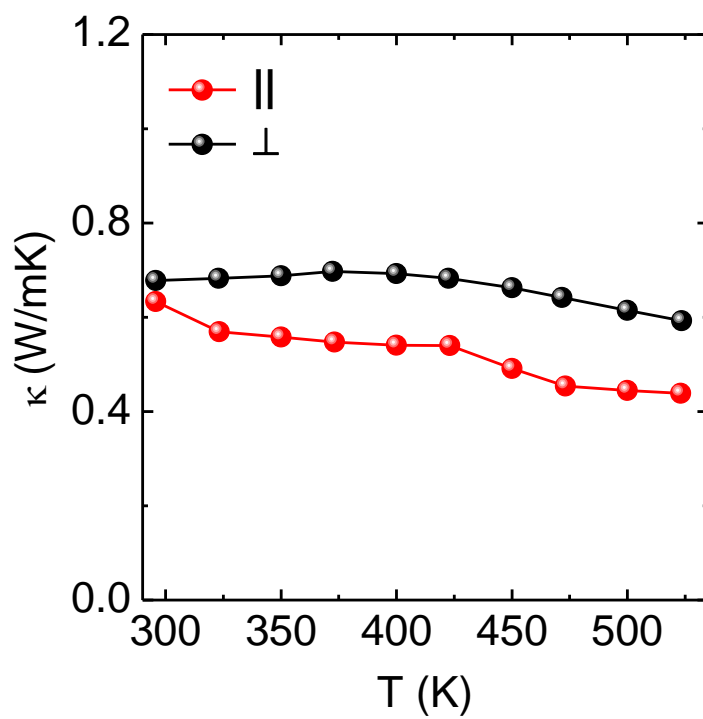


Figure S2. Total thermal conductivity (κ) of TlSe in parallel and perpendicular to pressing directions.

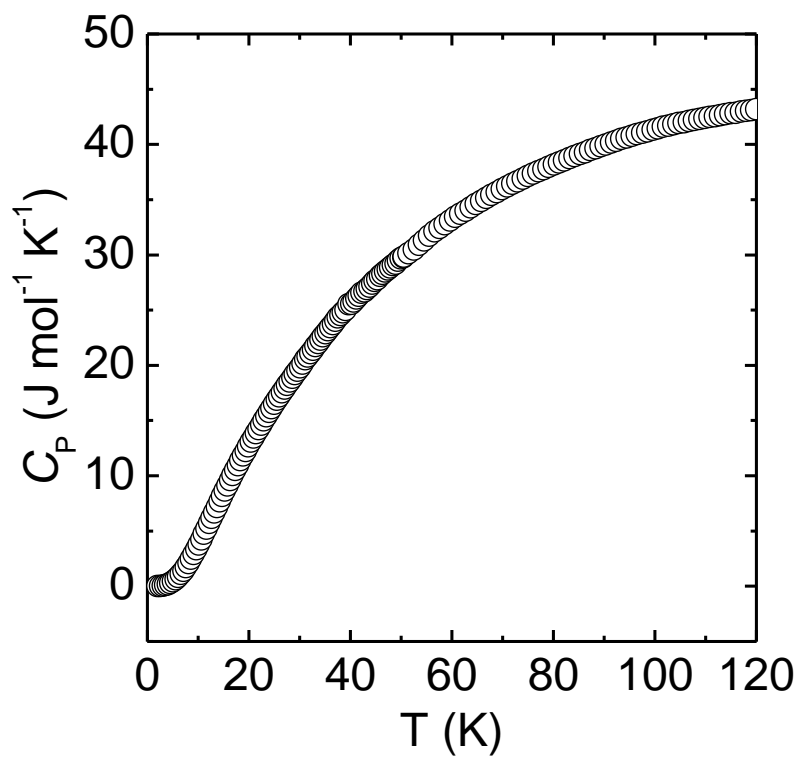


Figure S3. Temperature dependent heat capacity (C_p).

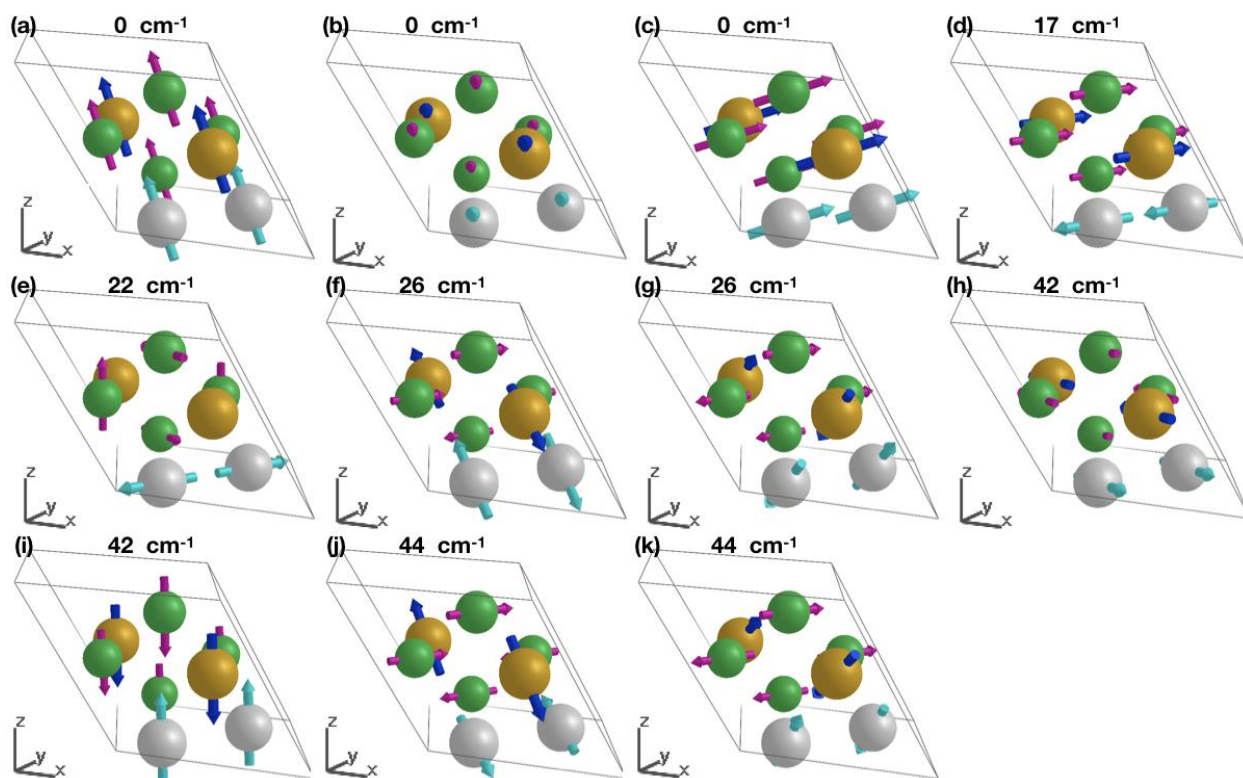


Figure S4. Eigen vector visualizations for the phonon modes at Γ point for 1 GPa case calculated using optimized lattice constant. Grey balls signify TI^+ , Gold balls represent TI^{3+} whereas Green balls signify Se atoms.

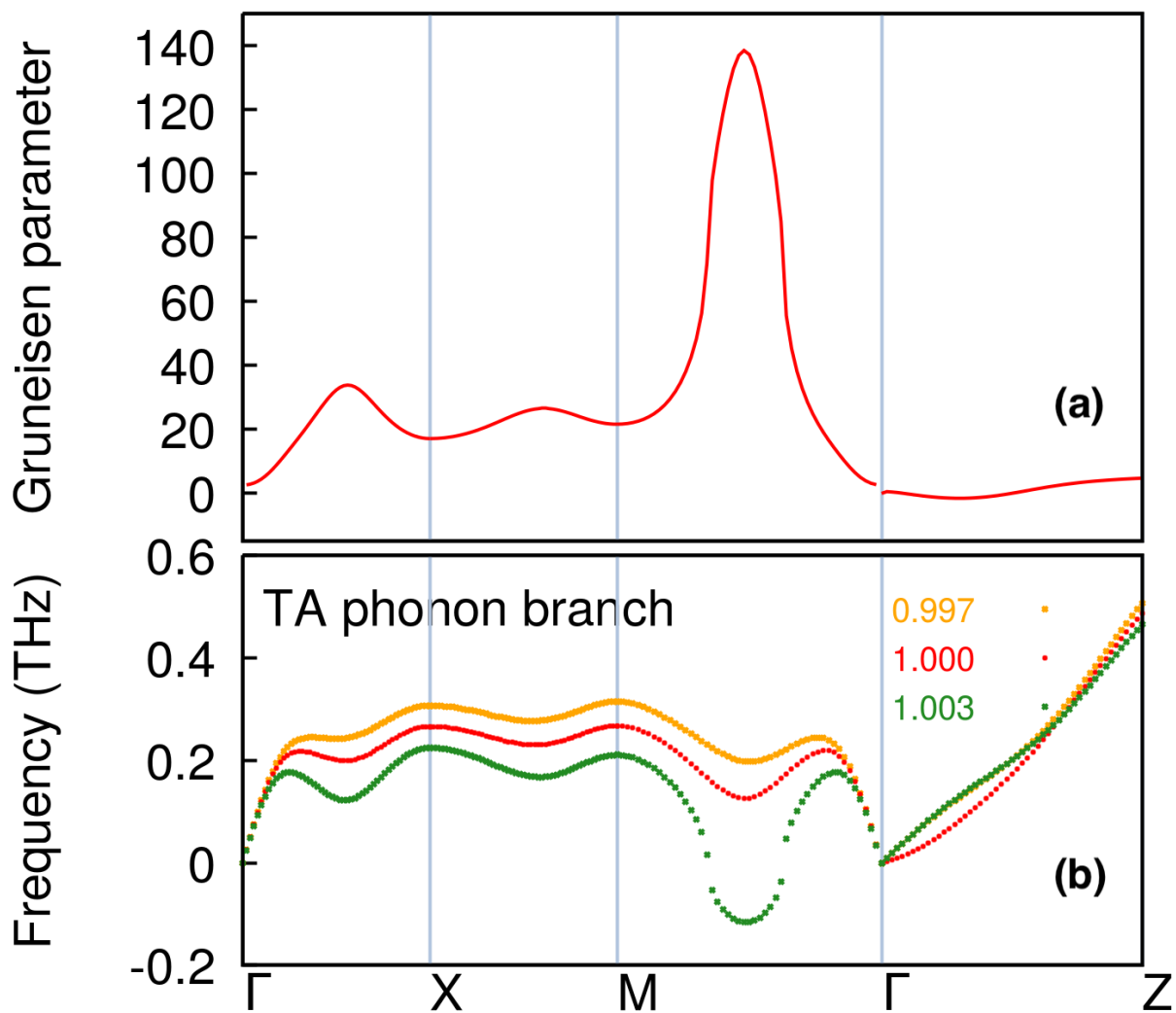


Figure S5. (a) Gruneisen parameters corresponding to the TA phonon branch ($P = 1$ GPa) of TlSe. (b) Sensitivity of dispersions of TA branch to the change in volume.

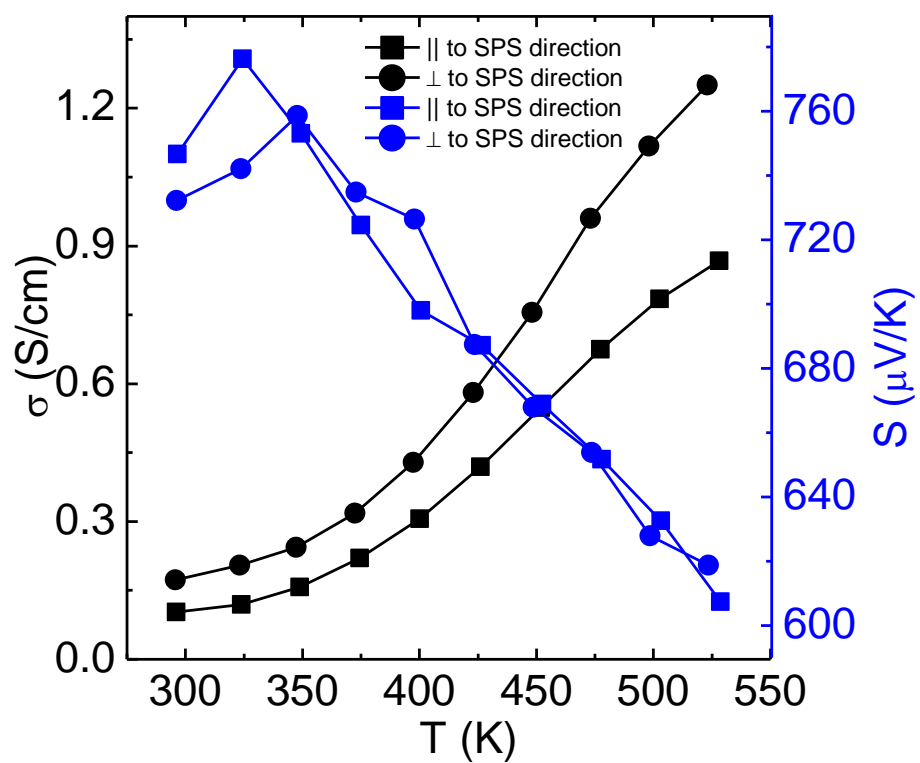


Figure S6. Temperature dependent Electrical Conductivity (σ) and Seebeck Co-efficient (S) of TlSe in parallel and perpendicular to the pressing direction of SPS.

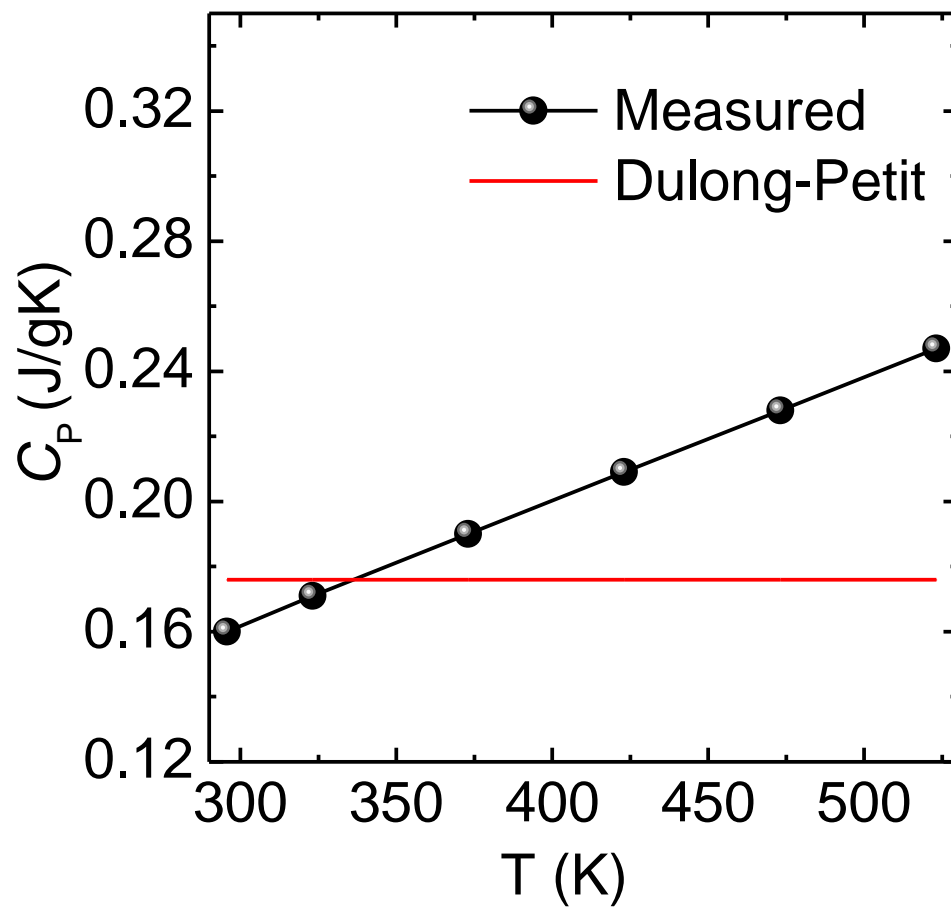


Figure S7. C_P measured using Pyroceram standard and Dulong-Petit calculated C_P .

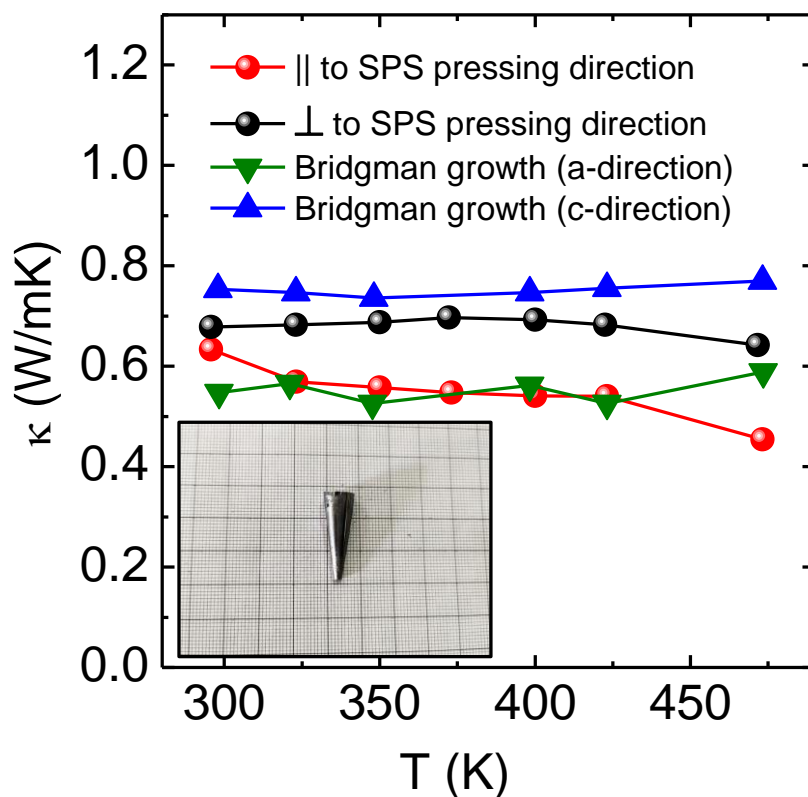


Figure S8. Comparison of thermal conductivity (κ) for Bridgman grown crystals and SPS sample. The density of Bridgman grown crystal is found to be only about 93% of the theoretical density, whereas the density of the SPS sample is ~99%. High density samples are the key for convincing thermal conductivity measurement. Thus, we have focused our analysis on SPS sample. Please note that, in 1968, Nayar *et al* have been reported κ_L of single crystal of TlSe to be ~90 to 40 W/mK in 300 to 520 K range,^{S7} which is unrealistic values for any heavy metal based selenides and tellurides.

Table S1. Reitveld refined structural parameters.

Space group: I4/mcm; a = b = 8.01171 (3) Å; c=6.96665 (2) Å; unit cell volume = 447.172 (2) Å ³ R _{wp} = 10.1 and χ^2 = 6.88						
Atom	x	y	z	Occupancy	Wyck.	U _{iso} (Å ²)
Se	0.18063	0.68063	0.00000	1.053	8h	0.015
Tl (1)	0.0	0.0	0.25	1.000	4a	0.026
Tl (2)	0.0	0.5	0.25	0.991	4b	0.023

Table S2. Parameters obtained after C_p fitting using 3 Einstein Oscillators.

Parameters	Values
$\gamma / \text{J mol}^{-1} \text{K}^{-2}$	$0.00483 \pm 9.91\text{E-}4$
$\beta / 10^{-4} \text{J mol}^{-1} \text{K}^{-2}$	$1.32 \pm 2.95\text{E-}3$
$\Theta_{\text{E1}}/\text{K}$	43.46 ± 2.32
$\Theta_{\text{E2}}/\text{K}$	22.74 ± 1.46
$\Theta_{\text{E3}}/\text{K}$	73.41 ± 4.72
A ₁	9.38 ± 1.32
A ₂	1.08 ± 0.29
A ₃	11.57 ± 0.82
Θ_{D} (K)	217 K
R ²	0.99999
χ^2	7.25E-7

Table S3. Parameters obtained after C_p fitting using 2 Einstein Oscillators.

Parameters	Values
$\gamma / \text{J mol}^{-1} \text{K}^{-2}$	$0.00796 \pm 1.08\text{E-}3$
$\beta / 10^{-4} \text{J mol}^{-1} \text{K}^{-2}$	$3.97 \pm 1.55\text{E-}1$
$\Theta_{\text{E1}}/\text{K}$	60.02 ± 0.89
$\Theta_{\text{E2}}/\text{K}$	31.32 ± 0.58
A_1	2.22 ± 0.03
A_2	0.54 ± 0.03
R^2	0.99994
χ^2	3.01E-6

Table S4. Parameters obtained after C_p fitting using 1 Einstein Oscillators.

Parameters	Values
$\gamma / \text{J mol}^{-1} \text{K}^{-2}$	0.0383 ± 0.00347
$\beta / 10^{-4} \text{J mol}^{-1} \text{K}^{-2}$	$5.87 \pm 1.62\text{E-}1$
$\Theta_{\text{E1}}/\text{K}$	47.08 ± 0.36
A_1	1.85 ± 0.029
R^2	0.99783
χ^2	6.75E-5

Table S5. Calculated zone centre phonon frequencies of TlSe.

0 GPa			1 GPa	
S. No.	Mode	Freq. (THz)	Mode	Freq. (THz)
1	A _{2u}	-0.0656	A _{2u}	0.1854
2	E _u	0.1898	E _u	0.2108
3	A _{2u}	0.3085	A _{2u}	0.5152
4	E _g	0.4866	A _{2g}	0.6547
5	A _{2g}	0.7735	E _g	0.7702
6	E _u	1.0804	E _u	1.2607
7	E _g	1.3273	E _g	1.3144
8	A _{2g}	2.0915	A _{2g}	2.3686
9	E _u	2.4182	E _u	2.5184
10	B _{1g}	2.6219	B _{1g}	2.7618
11	B _{2g}	2.8815	B _{2g}	2.8737
12	A _{2u}	4.2950	A _{2u}	4.3368
13	B _{1u}	4.3106	B _{1u}	4.3442
14	E _g	4.4984	E _g	4.5926
15	A _{1g}	5.1316	A _{1g}	5.1186
16	E _u	5.2448	E _u	5.3162
17	B _{2g}	6.1214	B _{2g}	6.2193

References.

- S1. Zhao, L.-D.; Lo, S.-H.; He, J.; Li, H.; Biswas, K.; Androulakis, J.; Wu, C.-I.; Hogan, T. P.; Chung, D.-Y.; Dravid, V. P.; Kanatzidis, M. G., High Performance Thermoelectrics from Earth-Abundant Materials: Enhanced Figure of Merit in PbS by Second Phase Nanostructures. *J. Am. Chem. Soc.* **2011**, *133*, 20476-20487.
- S2. (a) Yettapu, G. R.; Talukdar, D.; Sarkar, S.; Swarnkar, A.; Nag, A.; Ghosh, P.; Mandal, P., Terahertz Conductivity within Colloidal CsPbBr₃ Perovskite Nanocrystals: Remarkably High Carrier Mobilities and Large Diffusion Lengths. *Nano Letters* **2016**, *16*, 4838-4848; (b) Sarkar, S.; Saha, D.; Banerjee, S.; Mukherjee, A.; Mandal, P., Broadband terahertz dielectric spectroscopy of alcohols. *Chem. Phys. Lett.* **2017**, *678*, 65-71.
- S3. Jepsen, P. U.; Cooke, D. G.; Koch, M., Terahertz spectroscopy and imaging - Modern techniques and applications. *Laser Photonics Rev.* **2011**, *5*, 124-166.
- S4. Giannozzi, P.; Baroni, S.; Bonini, N.; Calandra, M.; Car, R.; Cavazzoni, C.; Ceresoli, D.; Chiarotti, G. L.; Cococcioni, M.; Dabo, I.; Dal Corso, A.; de Gironcoli, S.; Fabris, S.; Fratesi, G.; Gebauer, R.; Gerstmann, U.; Gougoussis, C.; Kokalj, A.; Lazzeri, M.; Martin-Samos, L.; Marzari, N.; Mauri, F.; Mazzarello, R.; Paolini, S.; Pasquarello, A.; Paulatto, L.; Sbraccia, C.; Scandolo, S.; Sclauzero, G.; Seitsonen, A. P.; Smogunov, A.; Umari, P.; Wentzcovitch, R. M., QUANTUM ESPRESSO: a modular and open-source software project for quantum simulations of materials. *J. Phys: Condens Matter* **2009**, *21*, 395502.
- S5. Monkhorst, H. J.; Pack, J. D., Special points for Brillouin-zone integrations. *Phys. Rev. B* **1976**, *13*, 5188-5192.
- S6. Cahill, D. G.; Watson, S. K.; Pohl, R. O., Lower limit to the thermal conductivity of disordered crystals. *Phys. Rev. B* **1992**, *46*, 6131-6140.
- S7. Nayar, P. S.; Verma, J. K. D.; Nag, B. D., Thermal Conductivity of Thallium Selenide. *J. Appl. Phys.* **1968**, *39*, 359-360.